

Supplementary data

Superior electrocatalytic performance of nitrogen-doped carbon-embedded Ni/NiO/NiB nanocrystals for urea oxidation

Xizi Zhao^{a*}

^a Data Science And Technology, North University of China, Taiyuan 030051, PR China

zhao_xi_zi@163.com (15834189196)

Table S1 Comparison of UOR performance of optimal samples in this work with relevant literature.

Catalysts	Potential @		Electrolyte	References
	10 mA cm ⁻² (V vs. RHE)	Tafel slope (mV dec ⁻¹)		
Ni/NiO/NiB@NC-500	1.38	48.73	1 M KOH + 0.33 M Urea	This work
Co ₃ O ₄ ^[1]	1.62	47	1 M KOH + 0.3 M Urea	2021
Cu ₃ P@CuO _x ^[2]	1.37	29	1 M KOH + 0.33 M Urea	2023
FeCo ₂ O ₄ @Co ₃ O ₄ ^[3]	1.387	67	1 M KOH + 0.3 M Urea	2023
CuO-Ni(OH) ₂ ^[4]	1.41	–	1 M KOH + 0.33 M Urea	2021
NiMo@ZnO/NF ^[5]	1.405	60.2	1 M KOH + 0.33 M Urea	2020
Co ₃ O ₄ /Ti ₃ C ₂ ^[6]	1.40	105	1 M KOH + 0.5 M Urea	2022
NC-FNCP ^[7]	1.37	51.2	1 M KOH + 0.5 M Urea	2022
H-NiFe-LDH/NF ^[8]	1.418	41.7	1 M KOH + 0.33 M Urea	2022
NiMoSe ^[9]	1.39	43.3	0.1 M KOH + 0.33 M Urea	2021
Fe ₃ O ₄ -NiO/NF ^[10]	1.44	32.5	1 M KOH + 0.33 M Urea	2020

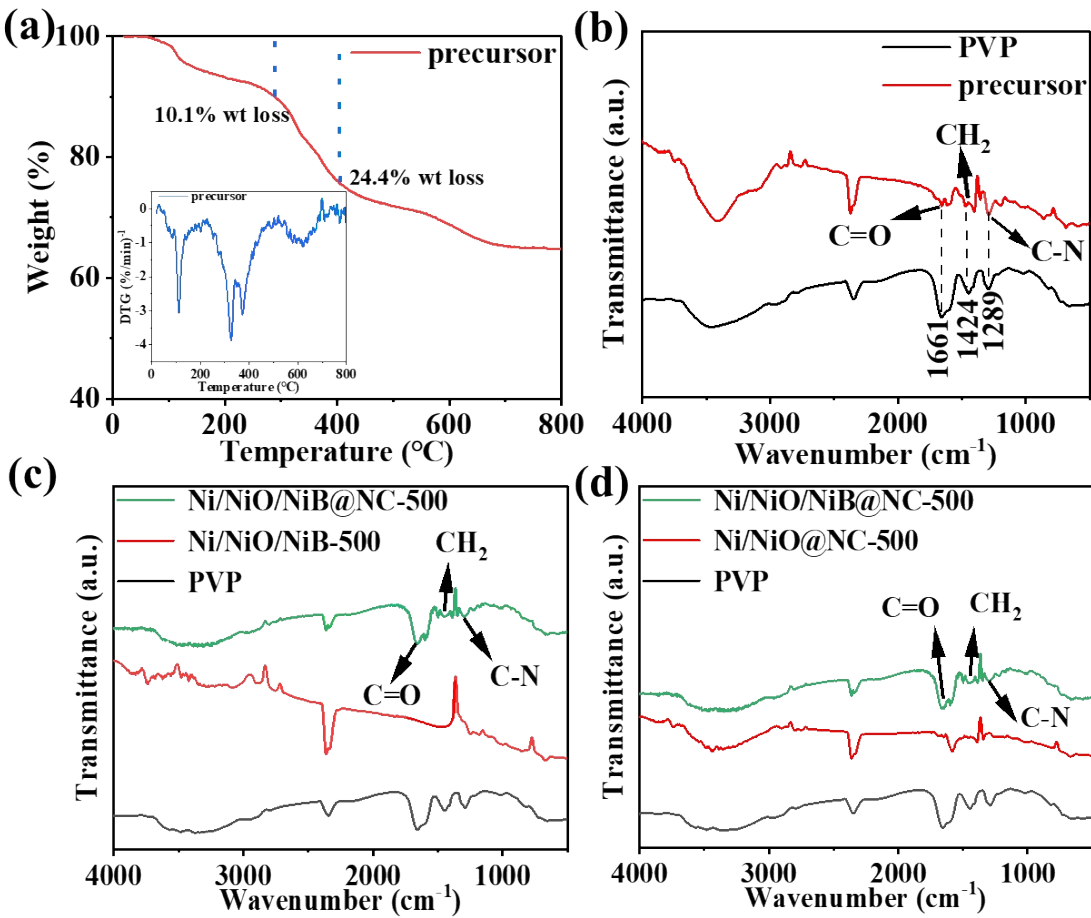


Fig. S1 (a) TGA and (Inset of Fig. S1a) DTG curves of the precursor. (b) FT-IR spectra of PVP and precursor, (c) PVP, Ni/NiO/NiB-500 and Ni/NiO@NC-500 and (d) PVP, Ni/NiO@NC-500, and Ni/NiO/NiB@NC-500.

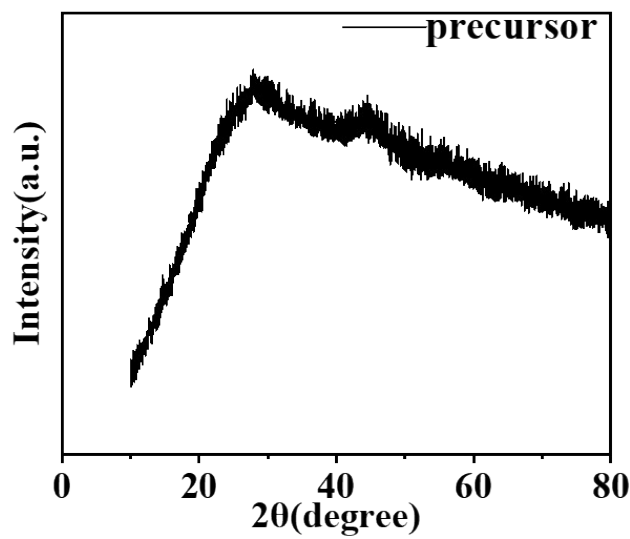


Fig. S2 XRD pattern of the precursor.

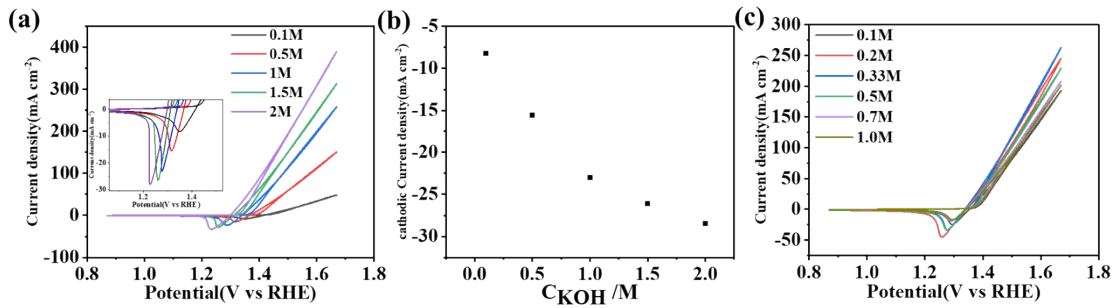


Fig. S3 (a) CV curves at a $50 \text{ mV}\cdot\text{s}^{-1}$ scanning rate with urea (0.33 M) and varying KOH concentrations. (b) Curve of cathode peak current density vs KOH concentration. (c) CV curves at a $50 \text{ mV}\cdot\text{s}^{-1}$ scanning rate with KOH (1.0 M) and varying urea concentrations.

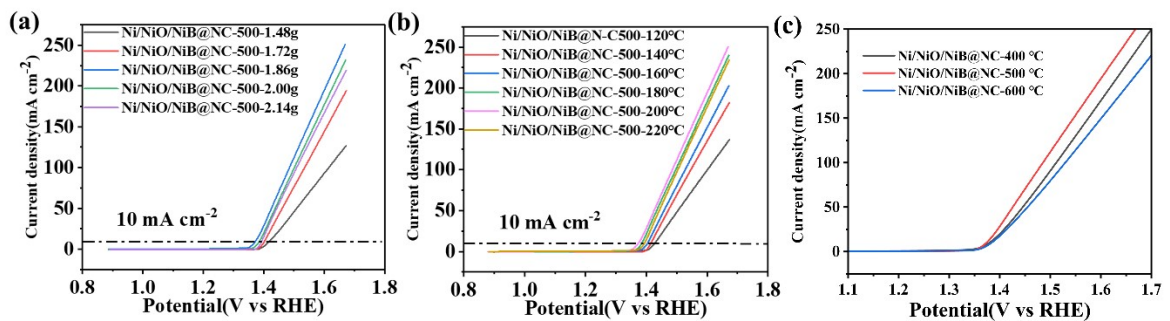


Fig. S4 (a) LSV curves of samples prepared at different boric acid concentrations in 1 M KOH + 0.33 M urea electrolyte. (b) LSV curves of samples prepared in different hydrothermal reaction temperatures in 1 M KOH + 0.33 M urea electrolyte. (c) LSV curves of samples prepared in different calcination temperatures in 1 M KOH + 0.33 M urea electrolyte.

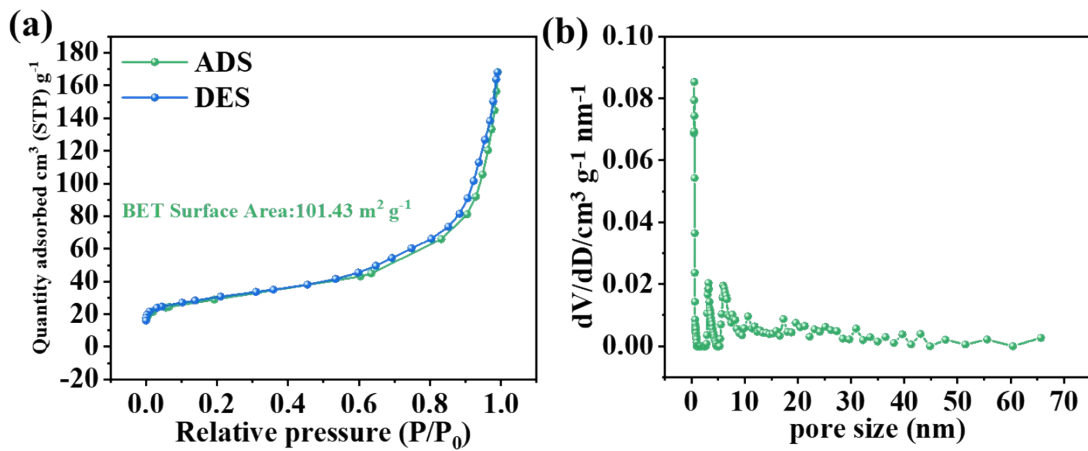


Fig. S5 (a) N_2 adsorption and desorption isothermal curves and (b) pore-size distribution curve of Ni/NiO/NiB@NC-500.

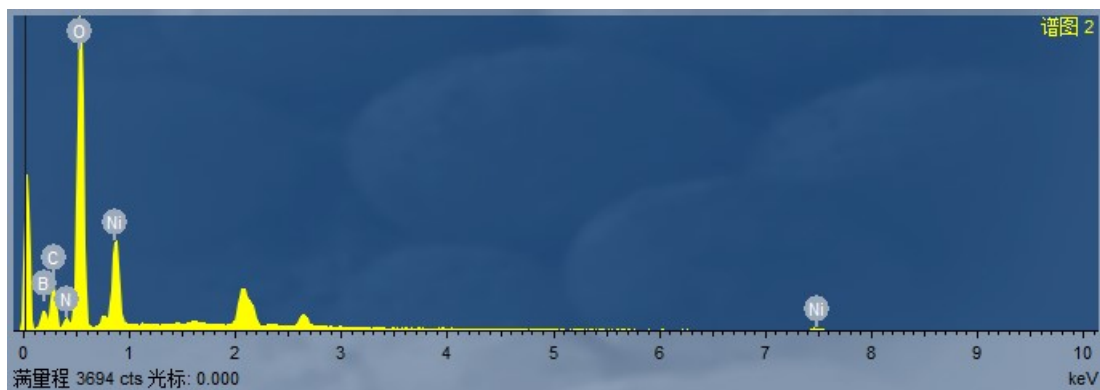


Fig. S6 EDS spectra of Ni/NiO/NiB@NC-500.

Element	Ling type	Percent (wt%)	Atomic percent
C	K series	13.30	18.32
O	K series	40.52	41.90
Ni	K series	23.91	6.74
N	K series	2.91	3.43
B	K series	19.36	29.62
Gross amount		100	

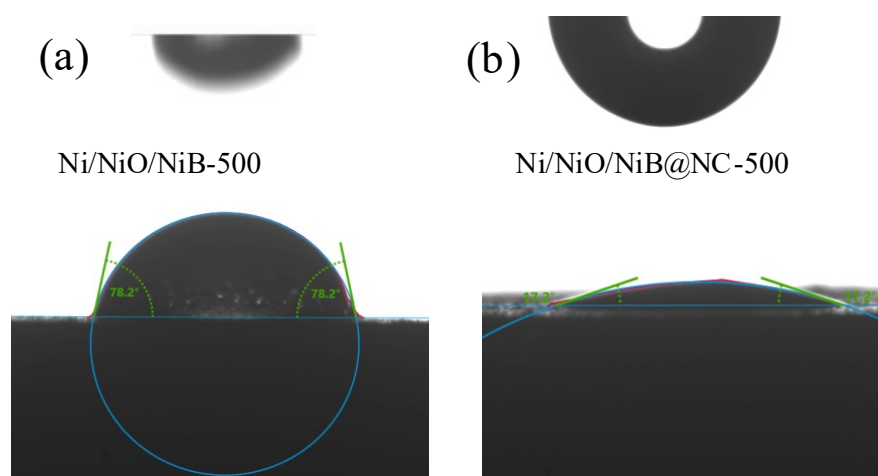


Fig. S7 Contact angle measurements of (a) Ni/NiO/NiB-500 and (b) Ni/NiO/NiB@NC-500.

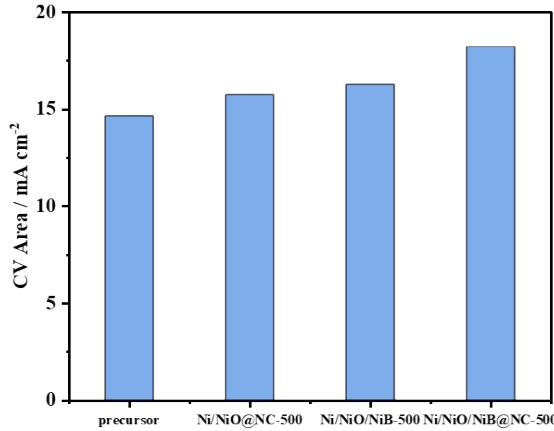


Fig. S8 (a) CV curve area comparison of different samples.

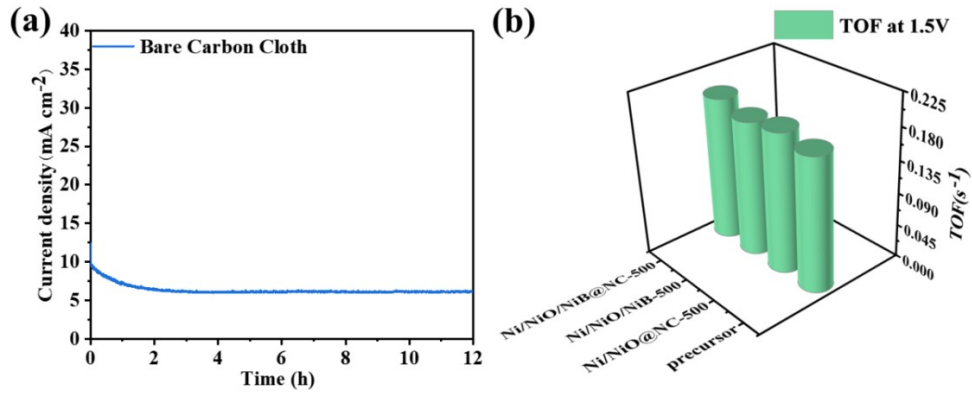


Fig. S9 (a) Long-term UOR test of bare carbon cloth at 1.6 V vs RHE in 1 M KOH with 0.33 M urea. (b) TOF values of precursor, Ni/NiO@NC-500 and Ni/NiO/NiB-500 and Ni/NiO/NiB@NC-500 at 1.5 V.

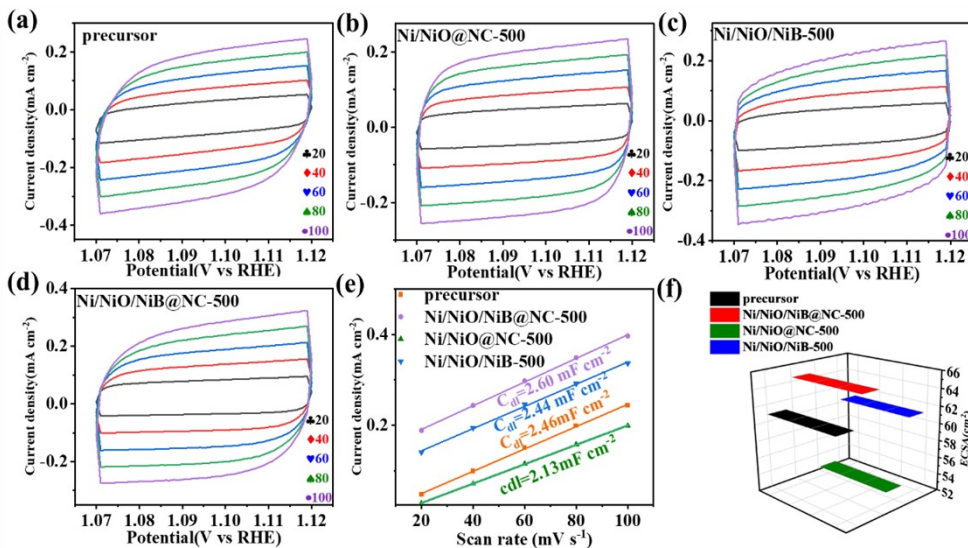


Fig. S10 CV curves of (a) precursor, (b) Ni/NiO@NC-500, (c) Ni/NiO/NiB-500 and (d) Ni/NiO/NiB@NC-500. (e) C_{dl} and (f) ECSA of different samples.

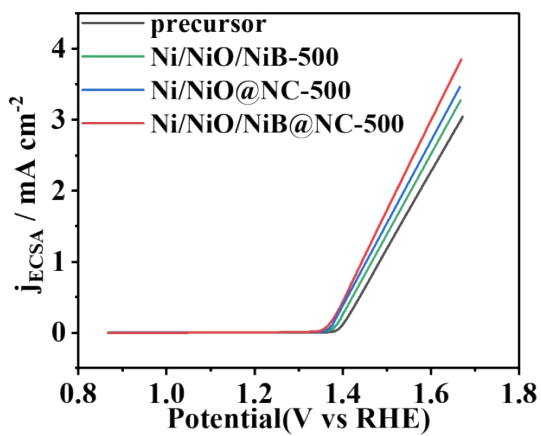


Fig. S11 UOR LSV curves normalized by ECSA.

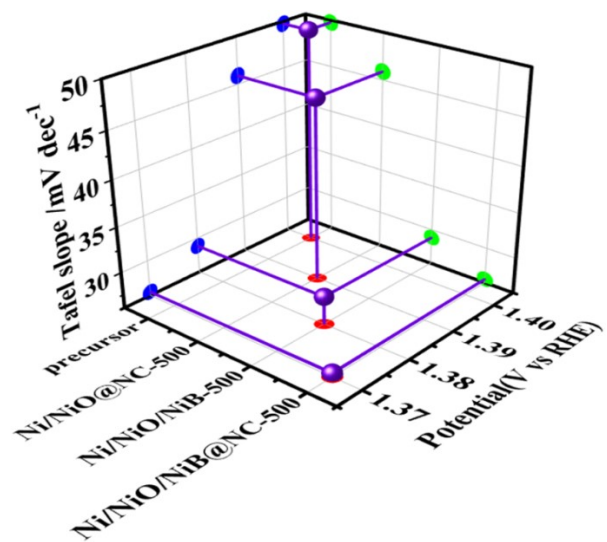


Fig. S12 Potentials required for UOR at 10 mA cm^{-2} and Tafel slopes of different samples.

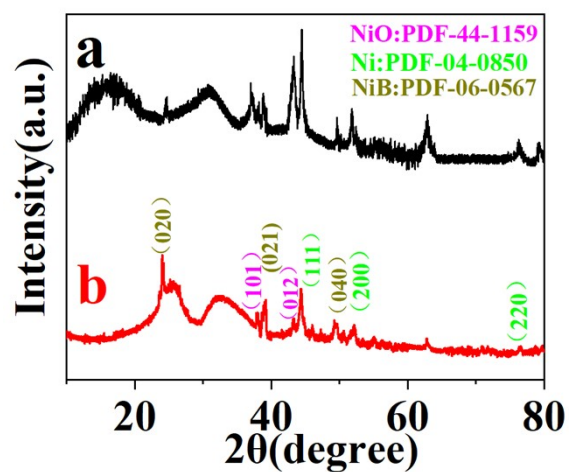


Fig. S13 XRD patterns of Ni/NiO/NiB@NC-500 samples (a) before and (b) after 12 h continuous CA tests.

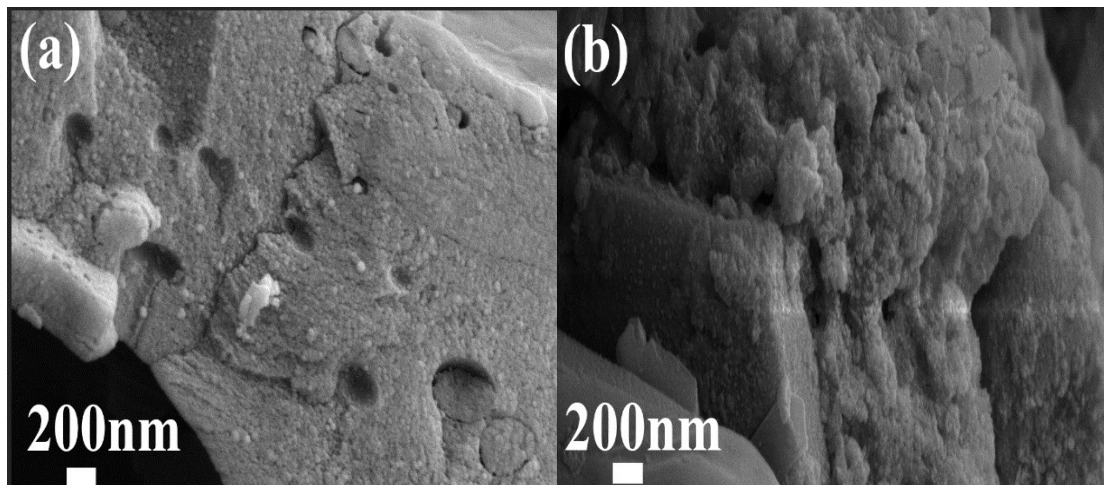


Fig. S14. SEM images of Ni/NiO/NiB@NC-500 (a) before and (b) after 12 h continuous CA tests.

Reference:

- [1] S. Li, J. Fan, S. Li, Y. Ma, J. Wu, H. Jin, Z. Chao, D. Pan, Z. Guo, In situ-grown Co_3O_4 nanorods on carbon cloth for efficient electrocatalytic oxidation of urea, *J. Nanostructure Chem.* 11 (2021) 735-749.
- [2] H.A. Bandal, H. Kim, In situ formed $\text{Cu}_3\text{P}@\text{CuO}_x$ as an efficient electrocatalyst for urea electrooxidation, *Appl. Surf. Sci.* 622 (2023) 156925.
- [3] S. Gao, J. Fan, G. Xiao, K. Cui, Z. Wang, T. Huang, Z. Tan, C. Niu, W. Luo, Z. Chao, Synthesis of $\text{FeCo}_2\text{O}_4@\text{Co}_3\text{O}_4$ nanocomposites and their electrochemical catalytical performances for energy-saving H_2 production, *Int. J. Hydrol. Energy* 48 (2023) 17147-17159.
- [4] J.-H. Yang, M. Chen, X. Xu, S. Jiang, Y. Zhang, Y. Wang, Y. Li, J. Zhang, D. Yang, CuO-Ni(OH)_2 nanosheets as effective electro-catalysts for urea oxidation, *Appl. Surf. Sci.* 560 (2021) 150009.
- [5] J. Cao, H. Li, R. Zhu, L. Ma, K. Zhou, Q. Wei, F. Luo, Improved hydrogen generation via a urea-assisted method over 3D hierarchical NiMo-based composite microrod arrays, *J. Alloy. Compd.* 844 (2020) 155382.
- [6] Y. Zhang, Z. Zhang, A. Addad, Q. Wang, P. Roussel, M.A. Amin, S. Szunerits, R. Boukherroub, 0D/2D $\text{Co}_3\text{O}_4/\text{Ti}_3\text{C}_2$ MXene Composite: A Dual-Functional Electrocatalyst for Energy-Saving Hydrogen Production and Urea Oxidation, *ACS Appl. Energy Mater.* 5 (2022) 15471-15482.
- [7] J. Zhang, S. Huang, P. Ning, P. Xin, Z. Chen, Q. Wang, K. Uvdal, Z. Hu, Nested hollow architectures of nitrogen-doped carbon-decorated Fe, Co, Ni-based phosphides for boosting water and urea electrolysis, *Nano Res.* 15 (2021) 1916-1925.
- [8] L. Chen, H. Wang, L. Tan, D. Qiao, X. Liu, Y. Wen, W. Hou, T. Zhan, PEO-PPO-PEO induced holey NiFe-LDH nanosheets on Ni foam for efficient overall water-splitting and urea electrolysis, *J. Colloid Interface Sci.* 618 (2022) 141-148.
- [9] H. Wang, X. Jiao, W. Zeng, Y. Zhang, Y. Jiao, Electrodeposition NiMoSe ternary nanoshperes on nickel foam as bifunctional electrocatalyst for urea electrolysis and hydrogen evolution reaction, *Int. J. Hydrol. Energy* 46 (2021) 37792-37801.
- [10] M. Han, G. Yan, Prussian blue analogue-derived porous bimetallic oxides $\text{Fe}_3\text{O}_4-\text{NiO}/\text{NF}$ as urea oxidation electrocatalysis, *Chem. Pap.* 74 (2020) 4473-4480.